Supporting Information

Determination of proline in human plasma samples using encapsulation of proline dehydrogenase enzyme in dendritic silica: A new platform for the enzymatic biosensing of amino acids

Arezoo Mirzaie [a], Arezoo Saadati [b], Soodabeh Hassanpour [c], Mohammad Hasanzadeh [c*], Mohammadreza Siahi-Shadbad [e], Abolghasem Jouyban [b]

[a] Student Research Committee, Faculty of pharmacy, Tabriz University of Medical Sciences, Tabriz, Iran

[b] Pharmaceutical Analysis Research Center and Faculty of Pharmacy, Tabriz University of Medical Sciences, Tabriz, Iran

[c] Drug Applied Research Center, Tabriz University of Medical Sciences, Tabriz, Iran

[d] Liver and Gastrointestinal Diseases Research Center, Tabriz University of Medical Sciences, Tabriz, Iran.

[e] Food and Drug Safety Research Center, Tabriz University of Medical Sciences, Tabriz, Iran.

Corresponding authors.
Drug Applied Research Center, Tabriz University of Medical Sciences, Tabriz, Iran
* hasanzadehm@tbzmed.ac.ir; mhmmd_hasanzadeh@yahoo.com

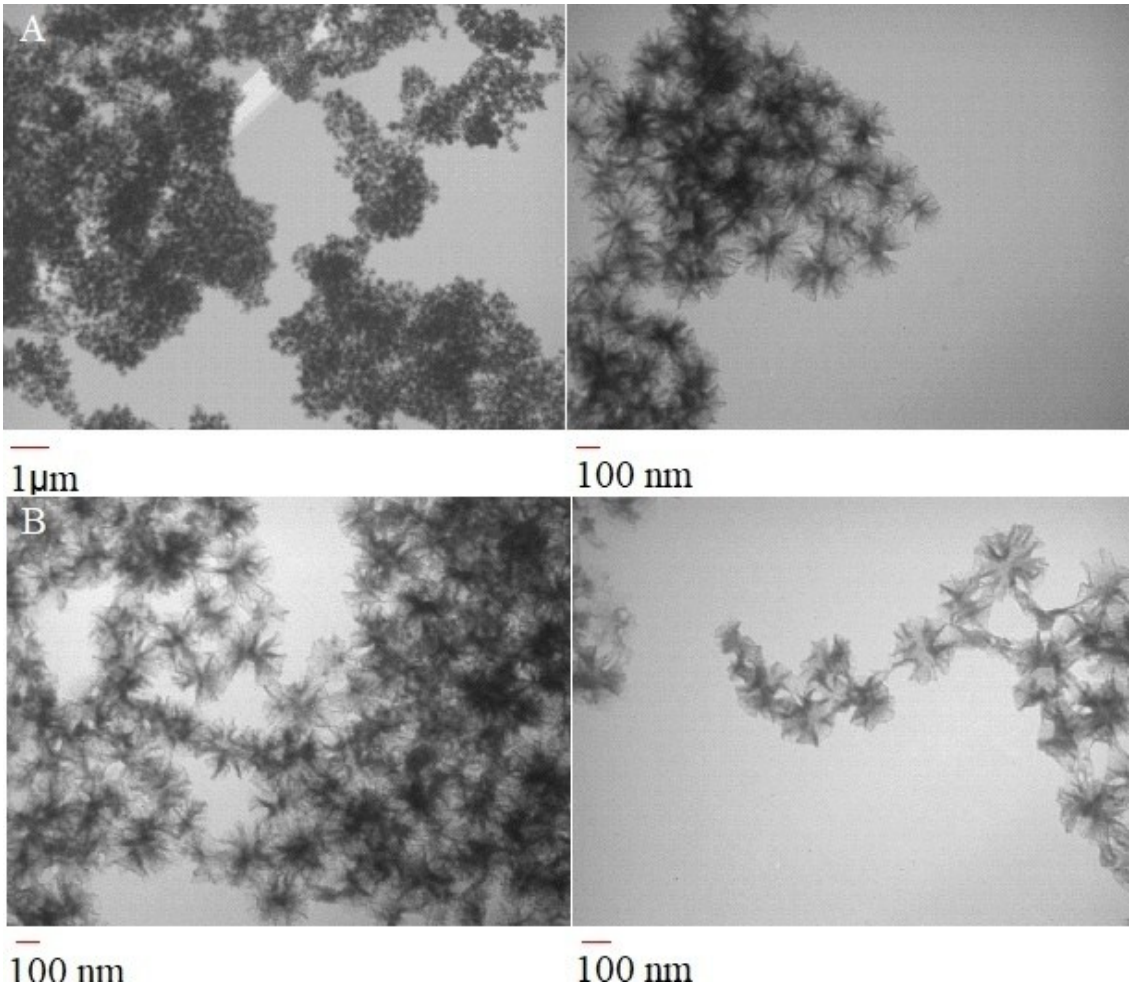

Fig. 1S. KCC-1 (A), KCC-1-NH_2 (B)

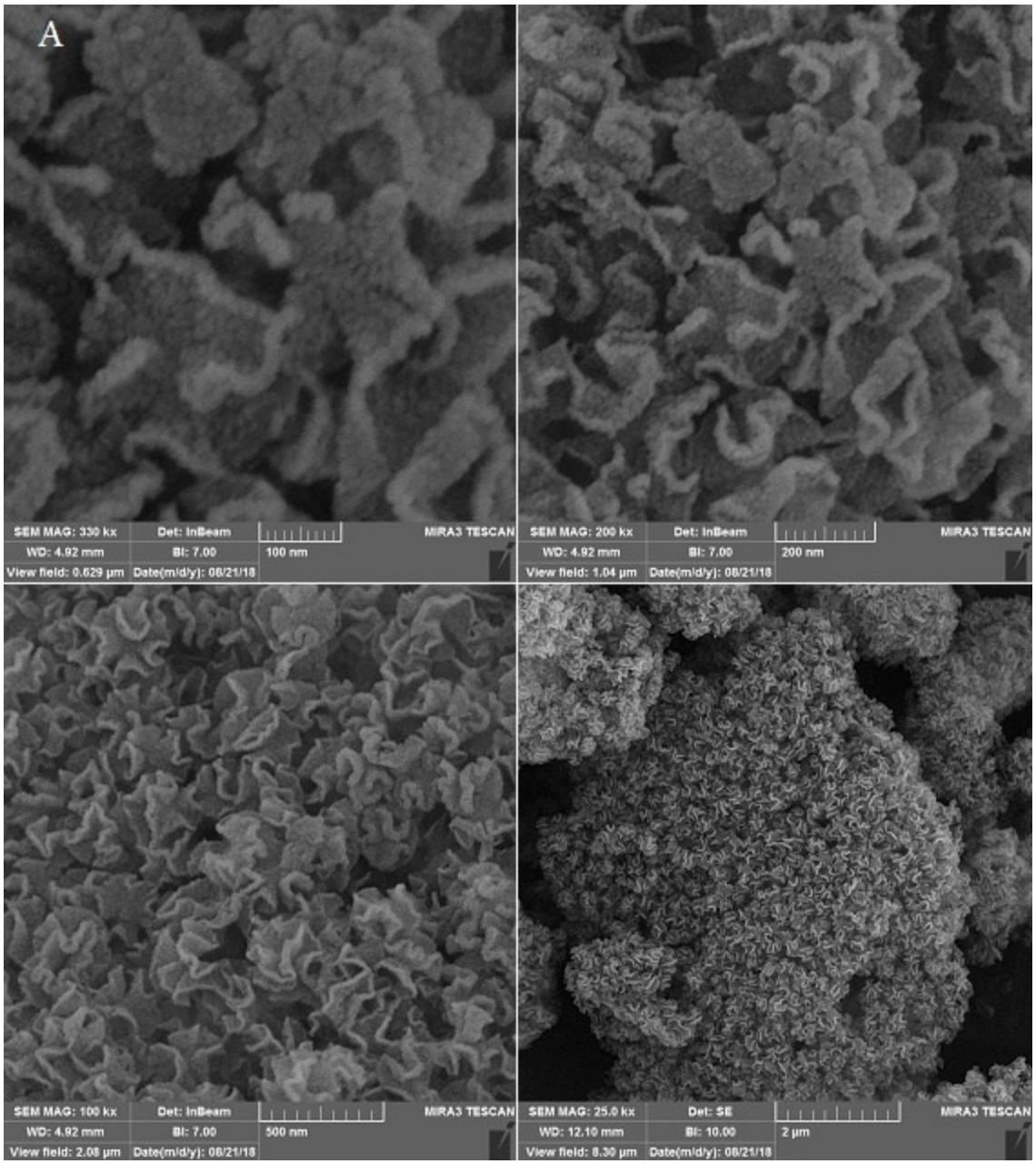
A
SEM MAG: 330 kx
Det: InBeam
MIRA3 TESCAN
WD: 4.92 mm
BI: 7.00
100 nm
View field: 0.629 µm
Date(m/d/y): 08/21/18
SEM MAG: 200 kx
Det: InBeam
MIRA3 TESCAN
WD: 4.92 mm
BI: 7.00
200 nm
View field: 1.04 µm
Date(m/d/y): 08/21/18
SEM MAG: 100 kx
Det: InBeam
MIRA3 TESCAN
WD: 4.92 mm
BI: 7.00
500 nm
View field: 2.08 µm
Date(m/d/y): 08/21/18
SEM MAG: 25.0 kx
Det: SE
MIRA3 TESCAN
WD: 12.10 mm
BI: 10.00
2 µm
View field: 8.30 µm
Date(m/d/y): 08/21/18

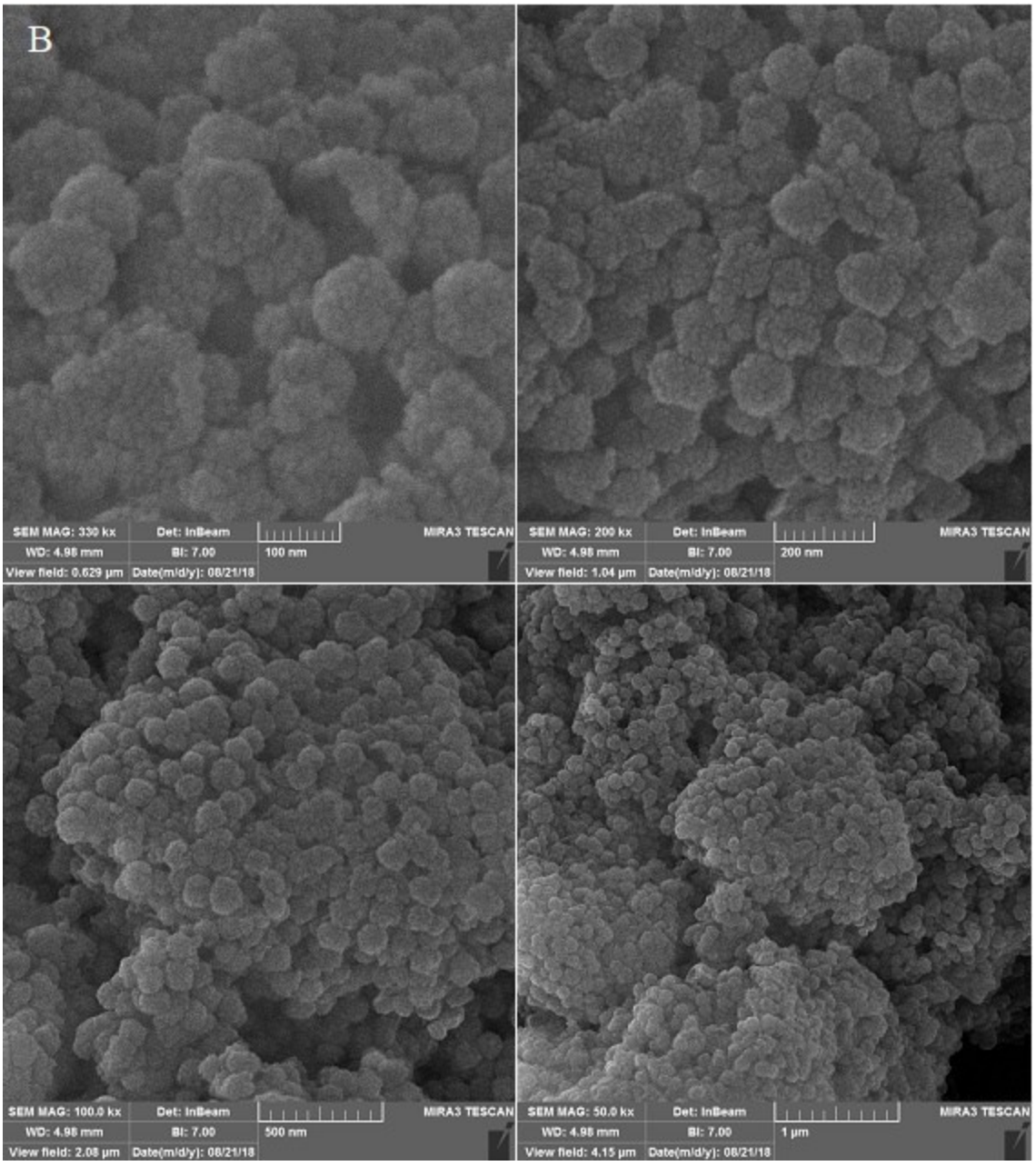

Fig. 2S. FE-SEM images of KCC-1 (A), KCC-1-NH_2 (B)

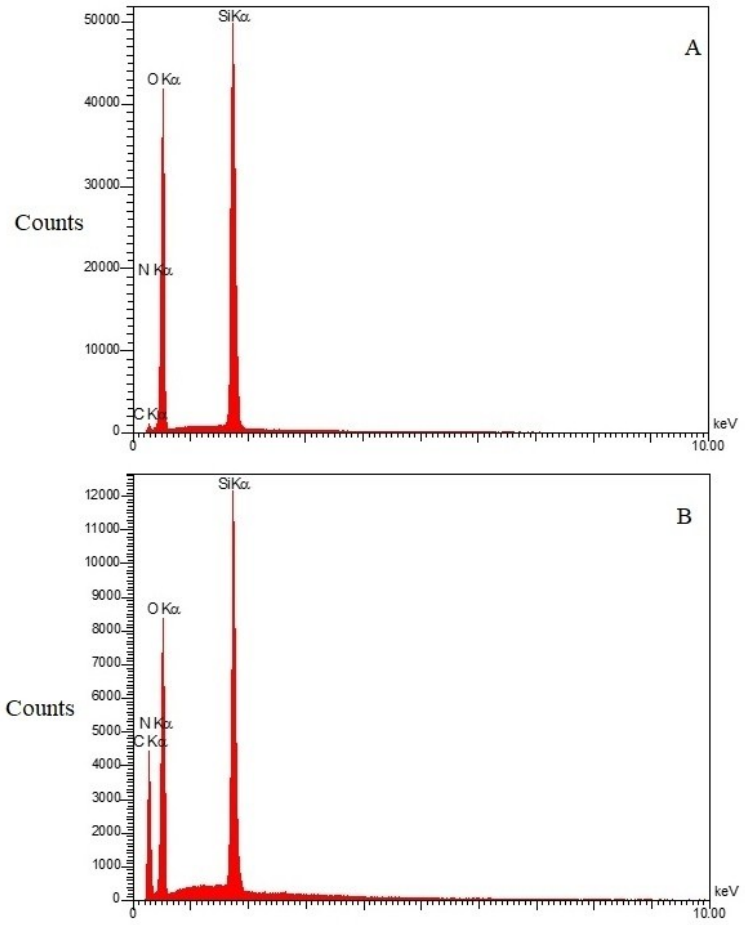

Fig. 3S. EDX analysis of KCC-1 (A), KCC-1-NH_2 (B)

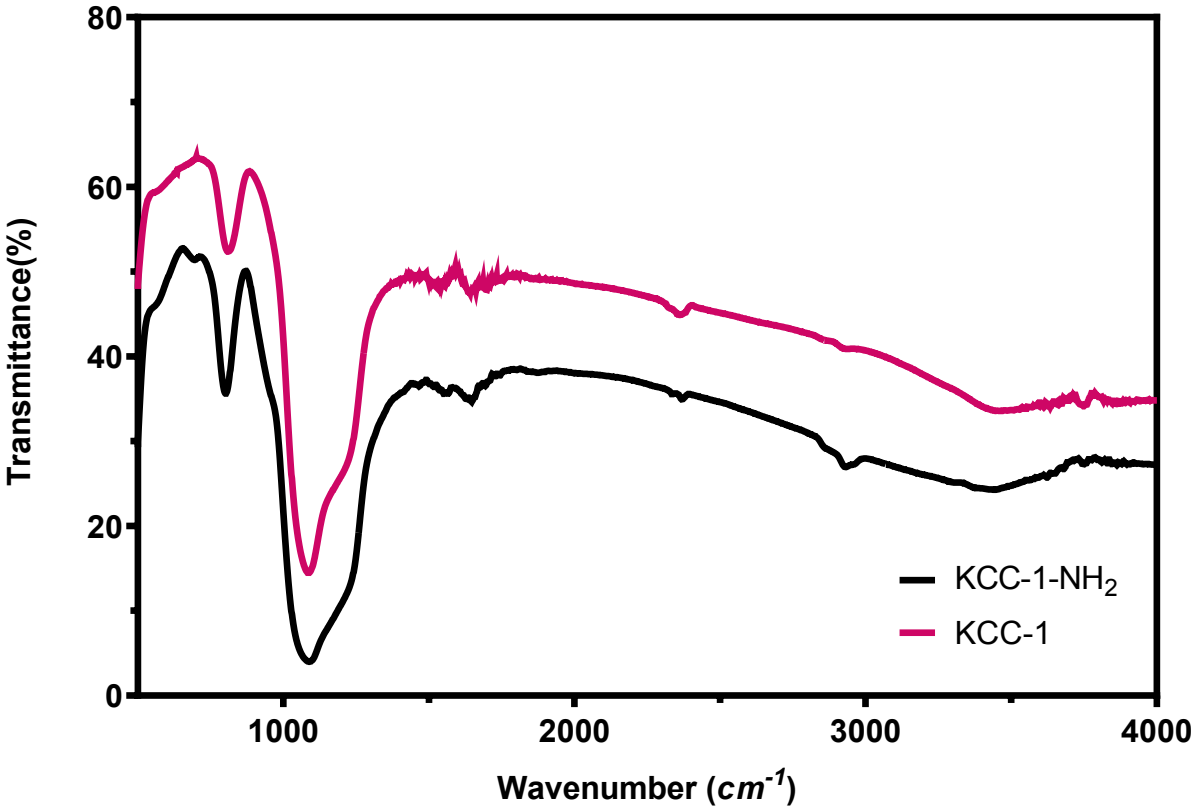

Fig. 4S. FTIR spectra of the KCC-1 and KCC-1-NH_2

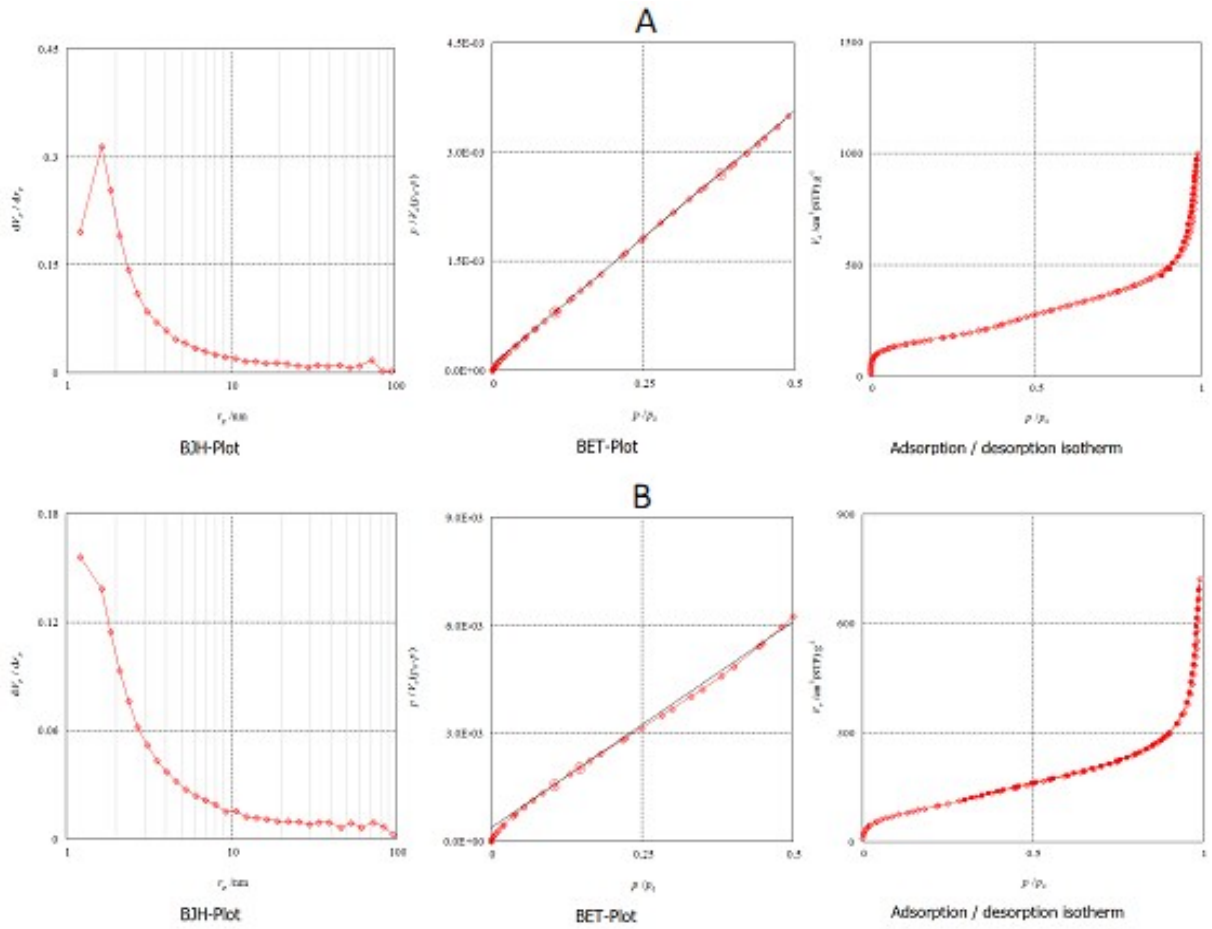

Fig. 5S. BJH, BET and nitrogen adsorption/desorption isotherm of KCC-1 (A), KCC-1-NH_2 (B). (P/P0= relative pressure (surface pressure/preliminary pressure)).

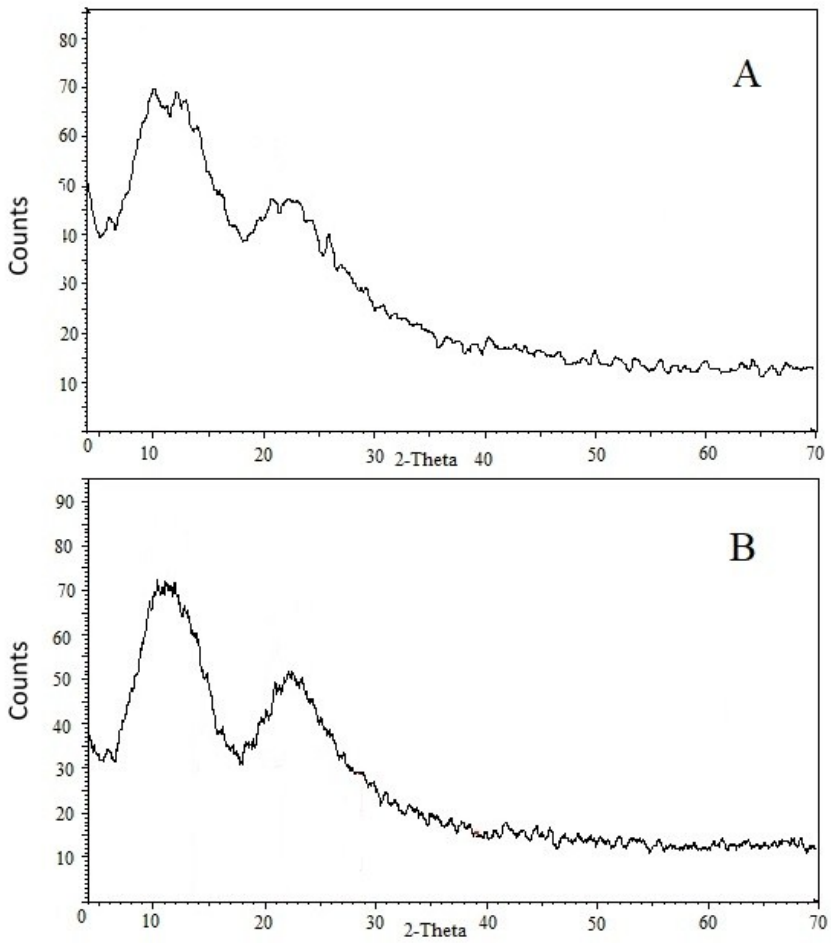

Fig. 6S. XRD analysis of KCC-1 (A), and KCC-1-NH_2 (B

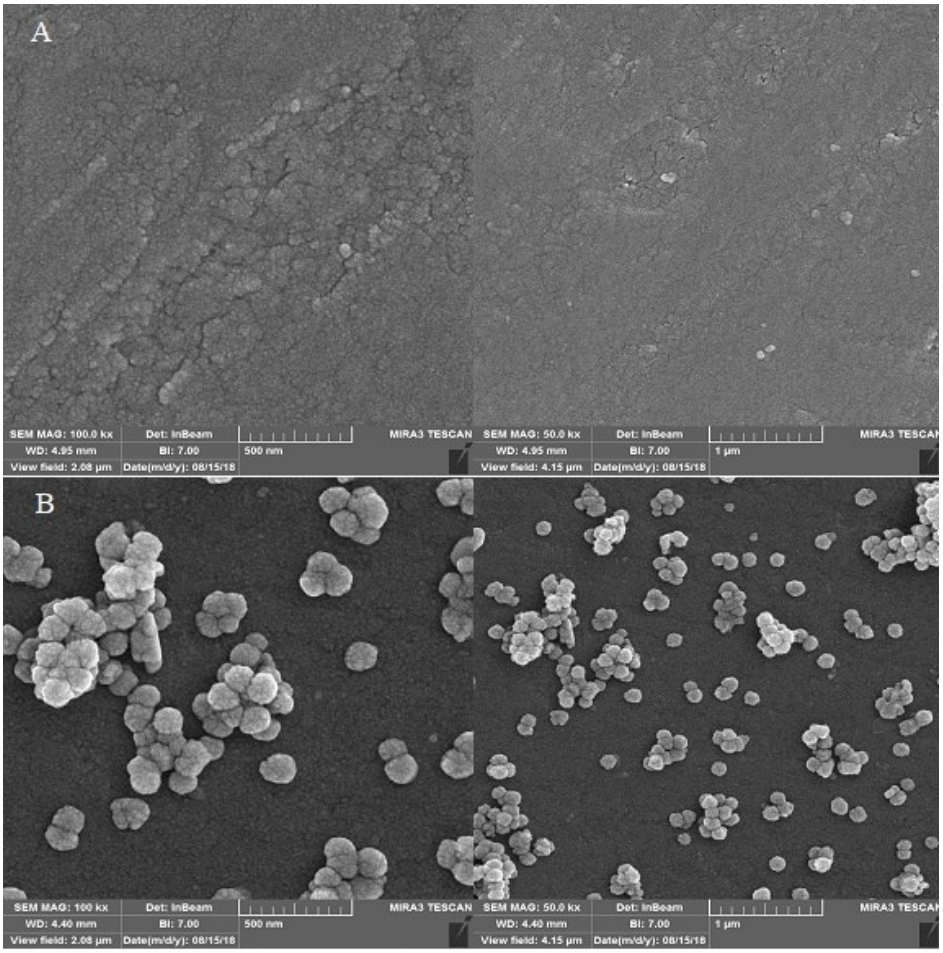

Fig. 7S. FESEM images of the KCC-1 (A), and KCC-1-NH_2 (B) modified GCE electrodes

Table 1S. Surface area, average pore size, and pore volume of KCC-1, and KCC-1-NH_2.

Material type	Pore size (nm)[a]	Pore volume ($cm^3\ g^{-1}$)[b]	Surface Area ($m^2\ g^{-1}$)
KCC-1	9.9	1.5	617
KCC-1-NH_2	11.9	1.1	367

a Pore size was calculated by BET. b Pore volume determined by BJH.

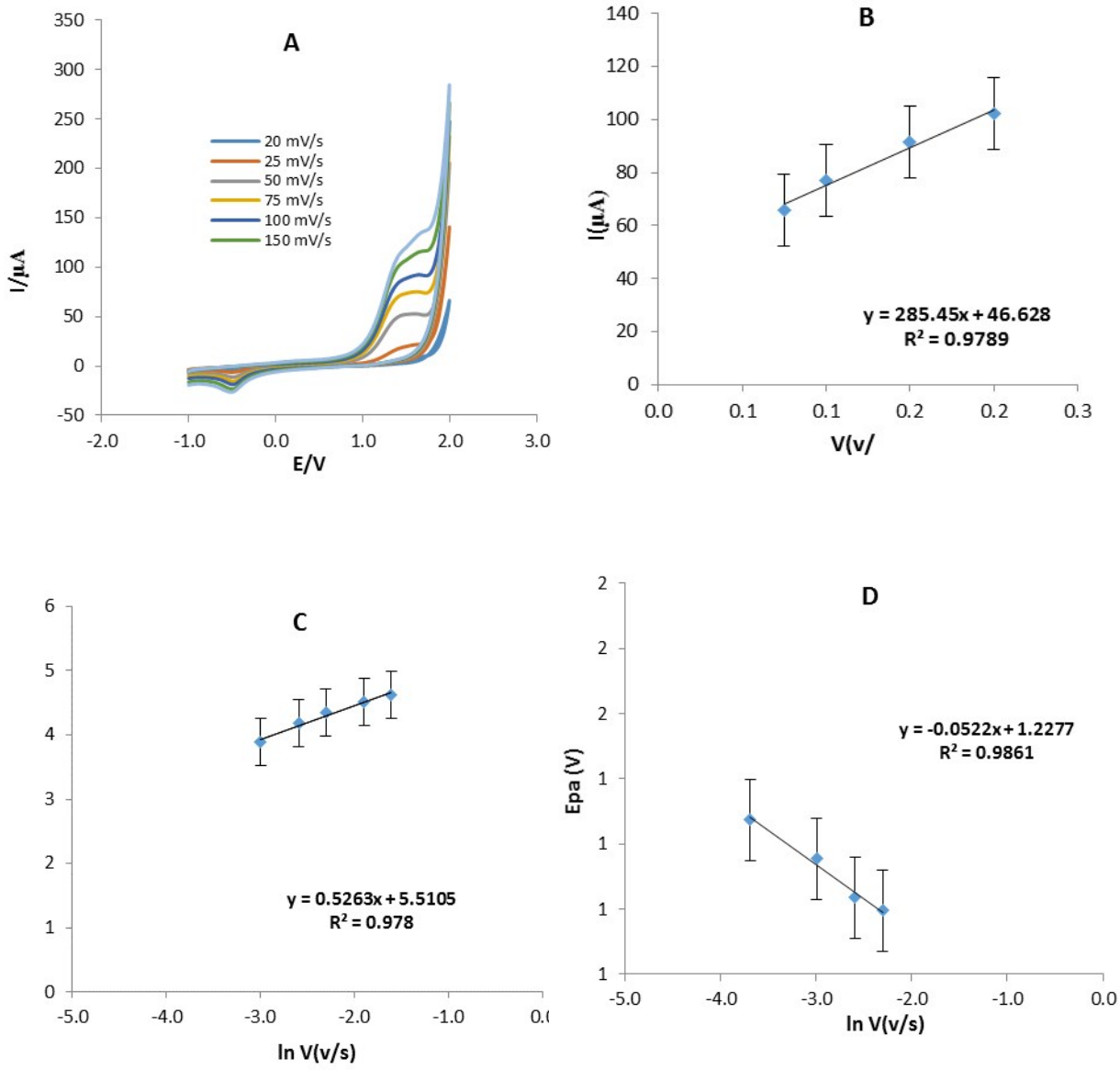

Fig. 8S. *(A) CVs of PRODH-KCC-1-NH_2-GCE in the presence of 34 mM of L-Pro in 0.1M PBS in different potential sweep rates (20-200mV/s). (B) Dependency of oxidation peak currents versus scan rates. (C) Variation of Ln I_{pa} versus Ln V. (D) The plot of oxidation peak potentials versus neperian logarithm of sweep rates.*

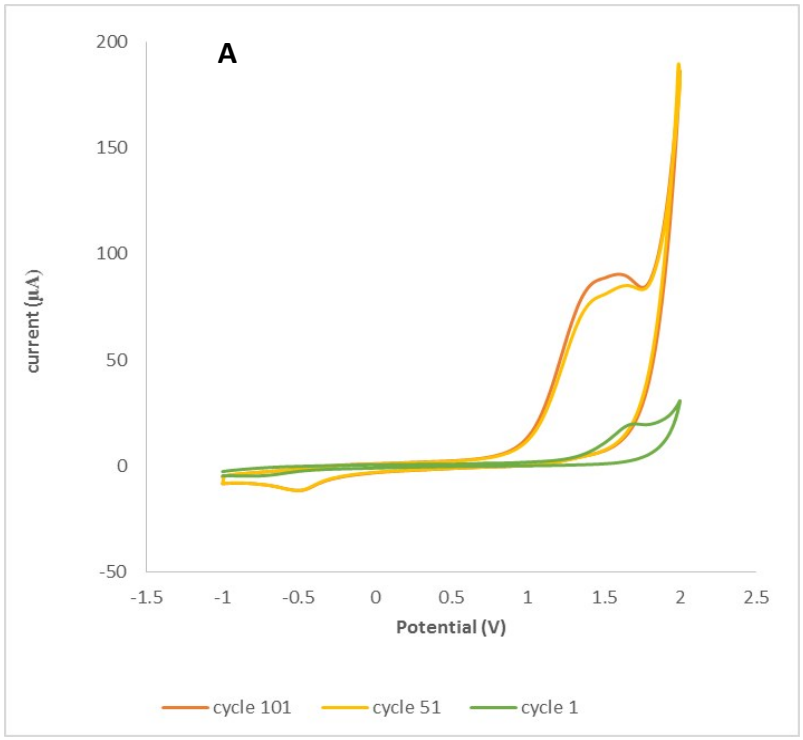
A
200
150
100
50
0
-50
current (µA)
-1.5
-1
-0.5
0
0.5
1
1.5
2
2.5
Potential (V)
cycle 101
cycle 51
cycle 1

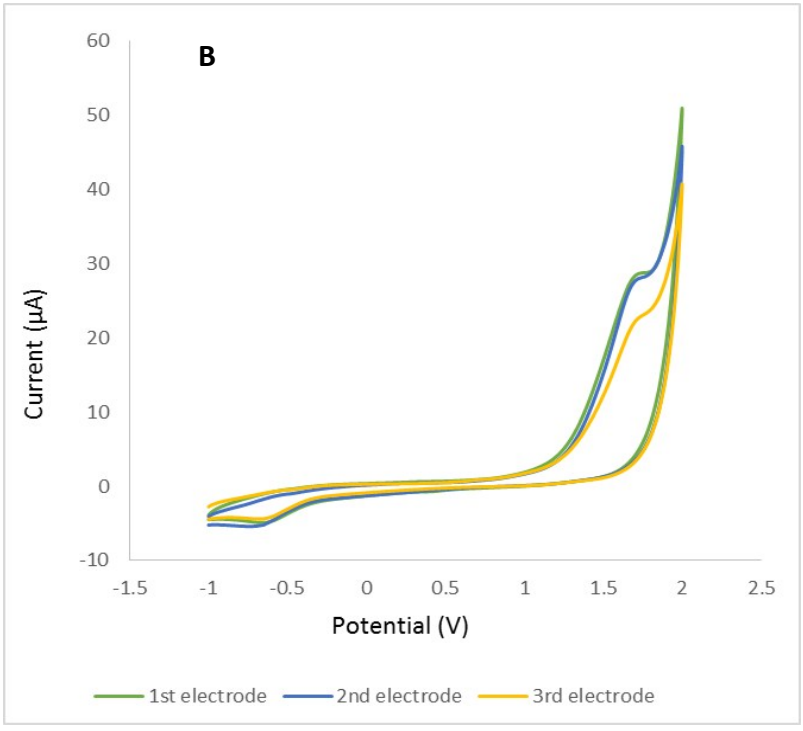
B
60
50
40
30
20
10
0
-10
Current (µA)
-1.5
-1
-0.5
0
0.5
1
1.5
2
2.5
Potential (V)
1st electrode
2nd electrode
3rd electrode

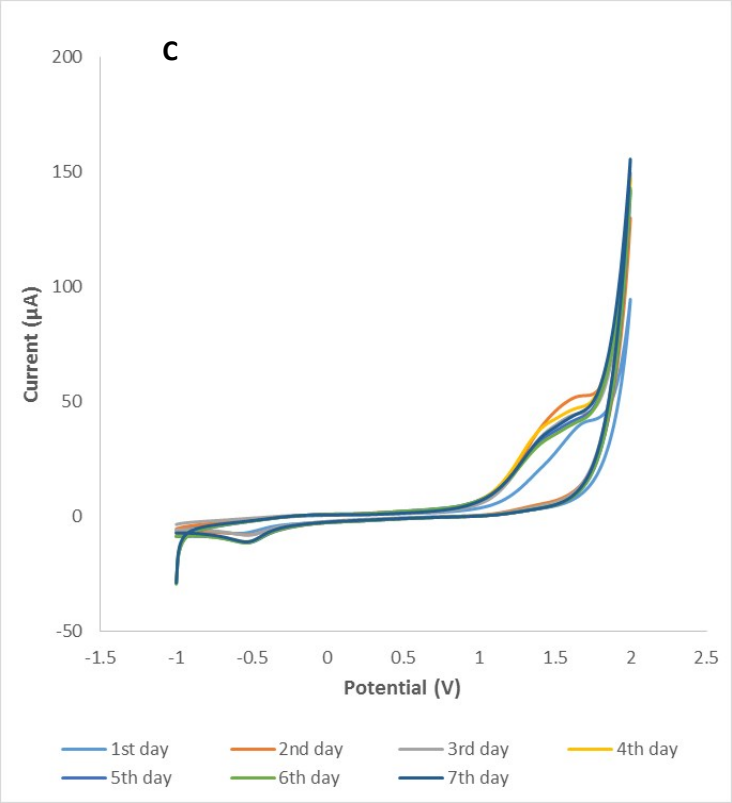

Fig. 9S: **A)** CVs of enzyme biosensor in different cycle number, **B)** CV of three similar enzyme biosensor with the same concentration of solution (supporting electrolyte) **C)** CV of enzyme biosensor in different time of storage.